

EVIDENCE OF INCREASED SURFACE EXPOSURE AND DIAGENETIC ALTERATION IN EVAPORITIC ENVIRONMENTS ON EARTH AND MARS. J. T. Haber¹, B. Horgan¹, S. Potter-McIntyre², A. Broz¹, R. Smith³, ¹Purdue University (haberj@purdue.edu), ²Southern Illinois University, ³Stony Brook University

Introduction: Sedimentary deposits in Gale and Jezero craters record a long-lived history of complex rock-water interactions (e.g. 1,2; Fig. 1) and understanding how the variable mineralogy of these deposits is linked to changing depositional and diagenetic environments in the Jezero delta and Mt. Sharp in Gale crater is important for constraining where to look for past habitable environments and signs of life with the Curiosity and Perseverance rovers.

While most rocks in the Murray formation in Gale crater appear to be fine-grained mudstones deposited in a deep lacustrine environment [3], we also see evidence of increased surface exposure in the form of mudcracks [Fig. 1; 4], evaporites [5], and clay mineral content [6,7]. Similar features have been observed at the Jezero delta front in Hogwallow Flats and Yori Pass [8], but their formation mechanisms and diagenetic history is still unclear. We look to similar features preserved in Carmel Formation on Earth to understand how the complex history of rock-water interactions on Mars is expressed in the rock record.

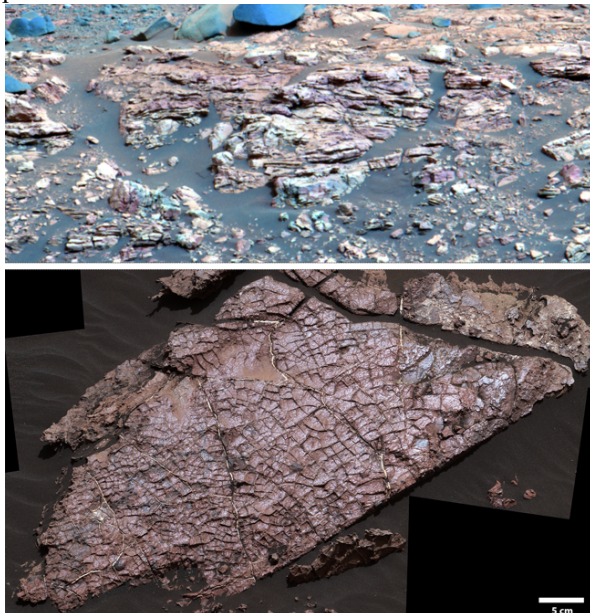


Fig. 1: Diagenetic mottling, concretions, and veins present in the Jezero delta (top; Mastcam-Z sol 613) and the Murray formation (bottom; Mastcam sol 1555) indicate that ground water was likely present after paleo-lakes dissipated.

The Jurassic Carmel Formation on Earth consists of carbonate- and sulfate-rich heterolithic strata deposited in a range of environments from fluvial, eolian, and coastal sabkha to shallow marine settings (Fig. 2; 9). The alteration mineralogy, variable sedimentology, and diagenetic features present makes this formation a good analog for parts of the Murray Formation in Gale crater

and stratigraphy at the Jezero delta front. Understanding how cementation and grain size affect the flow of diagenetic fluids, which can preserve or destroy biosignatures will help guide the search for signs of ancient life with Mars 2020. In this study, we look at how changes in lake level and climate manifest themselves in diagenetic features, chemistry, and mineralogy in the Carmel formation and how similar features may appear in Gale and Jezero craters.

Carmel Formation: In the ~25 m package of the Carmel exposed at Justensen Flats (Fig. 2), we observe depositional environments consistent with a shallow lacustrine or marine setting with fluvial/aeolian input and fluctuating water levels [9]. Finer-grained mudstones and siltstones were likely deposited in a low energy lacustrine setting while sandstones with small crossbeds may represent higher energy nearshore environments or even fluvial/aeolian deposition. Increasing evaporite content upsection into a cap of thick evaporite beds points to the drying out of this region and a transition from a shallow marine to a more nearshore or sabkha environment. Diagenetic features including Fe-oxide nodules, mottling, and gypsum veins are more common in strata deposited in nearshore environments.

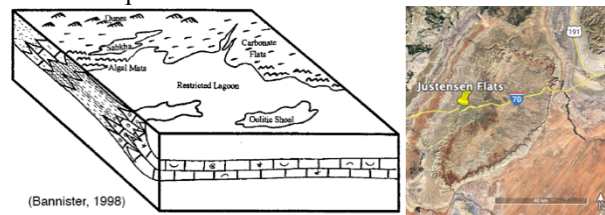


Fig. 2: Justensen Flats in the San Rafael Swell in Utah preserves several meters of Carmel stratigraphy deposited in a range of environments [9].

Methods: We collected visible/near-infrared (VNIR) spectra and samples from representative sections of the Jurassic Carmel Formation (Fig. 3) to see how changes in depositional environment are reflected in composition. Thin sections were made from a subset of samples and were analyzed using Scanning Electron Microscopy (SEM) with Energy Dispersive X-ray spectroscopy (EDS; Fig. 4) to determine mineralogy and diagenetic history [10].

Results: Carmel stratigraphy show variable depositional environments (Fig. 2) and diagenetic features that likely reflects multiple episodes of fluid flow as well as increased surface weathering and possible pedogenesis. VNIR spectra (Fig. 3) of a section of maximum transgression show changes in composition related to bedrock color and sedimentology. Spectra from the Navajo sandstone below the Carmel are consistent with sandstone cemented by kaolinite while most of the Carmel

appears to be cemented by carbonates, such as dolomite. Gray and green bedrock (Fig. 3D) exhibits a peak at ~ 575 nm, a sharp absorption at ~ 750 nm, and a broad absorption at ~ 1100 nm, consistent with mixed valence Fe-bearing clays and carbonates. Gypsum is present as chicken-wire massive deposits, diagenetic veins (Fig. 3B), and concretions and is indicated by the triplet near $1.4 \mu\text{m}$, a band at $1.75 \mu\text{m}$, and a doublet with local minima at $2.21\text{--}2.27 \mu\text{m}$ [11]. Dark red/purple mudstone (Fig. 3C) exhibits absorptions at ~ 550 nm and ~ 860 nm indicative of Fe-oxides such as hematite [12], which is also present as mm-scale concretions.

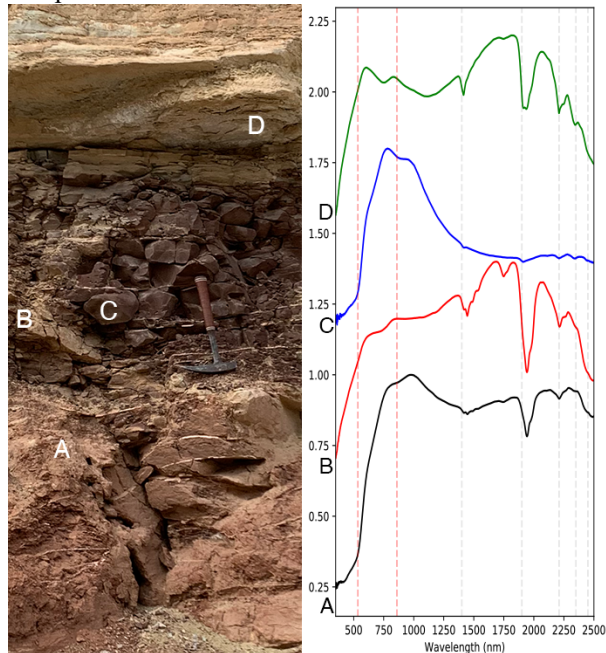


Fig. 3: Section of the Carmel Formation at the end of a transgressive cycle where red/purple mudstones crosscut by diagenetic veins are topped by a thick bed of chicken-wire gypsum. Changes in mineralogy, including clays, carbonates, evaporites, and Fe-oxides, are reflected in VNIR spectra. Vertical lines indicate absorptions associated with relevant minerals.

SEM/EDS Results: Microscopy shows diverse mineralogy that is consistent with VNIR spectra. Carbonate cement is pervasive, even in nearshore deposits, but is less present in bleached bedrock (Fig. 4). Differences in permeability, grain size, and cementation likely caused diagenetic fluids to preferentially bleach less cemented regions of bedrock causing the rock to appear mottled (Fig. 3). Additional analysis will help determine the relative timing of diagenesis and how mineralogy changes throughout this section.

Implications: The variable sedimentology and evaporite content in the Carmel suggests changing water level due to climatic influence. Increased surface exposure likely led to more oxidation and evaporite content during periods of low water levels. Clay content and possible pedogenic alteration could also be due to surface exposure and weathering.

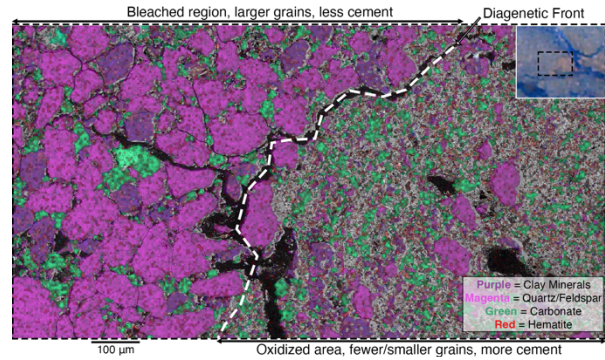


Fig. 4: SEM/EDS results from a sample displaying diagenetic mottling shows differences in cementation and grain size between the bleached (left) and oxidized (right) regions. Minerals are interpreted from EDS data.

Parts of the Jezero delta front stratigraphy, such as Yori Pass and Hogwallow Flats, exhibit mottling (Fig. 1), concretions, and veins that could be due to multiple episodes of diagenesis [8]. Additionally, bedrock in this region appears enriched in sulfates including hydrated and anhydrous Ca-sulfates and Fe-Mg-sulfates. Both primary sulfates and diagenetic cements can potentially trap and preserve biosignatures in their crystal structure [13] and are major targets for Mars sample return.

Similar diagenetic features [Fig. 1] and bedrock sulfate enrichment [5] is found in parts of Mt. Sharp, including the Sutton Island member of the Murray Formation [5,7] and the clay-sulfate transition. These regions are hypothesized to have been deposited in a more nearshore or lowstand environment with increased surface exposure.

In addition to the bed of massive gypsum in the Carmel, gypsum veins are present along fractures and bedding planes throughout the section. These can provide a pathway for diagenetic fluids, even in relatively impermeable fine-grained rocks, and may affect biosignature preservation on Mars. Preliminary comparison of evaporite veins in the Uganik Island abrasion target in Yori Pass show veins cross-cutting rocks and are mostly Ca-sulfate bearing [14]. Future work will focus on analyzing analog gypsum vein fabrics that will be compared to rover observations and returned samples from the Jezero delta.

References: [1] Grotzinger et al. (2014) *Science* 343 [2] Horgan et al. (2020) *JGR* 125 [3] Fedo et al. (2019) *Mars* 9 6308 [4] Stein et al. (2018) *Geol.* 46 6 [5] Rapin et al. (2019) *Nature Geo.* 12 [6] Bristow et al. (2018) *Science* 4 eaar3330 [7] Haber et al. (2022) *JGR* 127 [8] Broz et al. this conf. [9] Blakey et al., (1983) *RMS* 2 [10] Potter-McIntyre et al. (2014) *JSR* 84 875-892 [11] Cloutis et al. (2006) *Icarus* 184 [12] Morris et al. (1989) *JGR* 94 2760 [13] Bennison et al. this conf. [14] Nachon et al. this conf.